April, 1998

Cellular Automaton Modeling of Alloy Solidification Using Local Anisotropy Rules

Ralph E. Napolitano
T. H. Sanders Jr., *Georgia Institute of Technology*

CELLULAR AUTOMATON MODELING OF ALLOY SOLIDIFICATION USING LOCAL ANISOTROPY RULES

R. E. NAPOLITANO* and T. H. SANDERS, JR.**
*Metallurgy Division, National Institute of Standards and Technology, Gaithersburg, MD, 20899
**Materials Science and Engineering, Georgia Institute of Technology, Atlanta, GA, 30332

ABSTRACT

The evolution of dendritic morphology is simulated for a binary alloy using a two-dimensional cellular automaton growth algorithm. Solute diffusion is modeled with an alternate-direction implicit finite difference technique. Interface curvature and kinetic anisotropy are implemented through configurational terms which are incorporated into the growth potential used by the automaton. The weighting of the anisotropy term is explored and shown to be essential for overcoming grid-induced anisotropy, permitting more realistic development of dendritic morphologies. Dendritic structures are generated for both uniform and directional cooling conditions.

INTRODUCTION

Virtually every microstructural feature in a cast alloy component is related to the interface morphology present during solidification. Conventional solidification theory, describing dendrite tip kinetics and mushy zone phenomena, provides a means for estimating overall microstructural parameters for an alloy solidified under steady-state conditions. Microstructural prediction for actual components, which are finite in size and complex in geometry, requires a description of the evolution of the interface morphology under transient conditions and geometrical constraint and an understanding of how the structure propagates through the mold. Any useful simulation tool must be equipped to handle these circumstances within the limits of computational feasibility.

Solidification involves the growth of a solid phase into a liquid phase, where the growth is controlled by the continuity of thermal and solutal fields along with energetic conditions at the interface. A major problem encountered in solidification modeling, however, is that the controlling phenomena operate at different size scales. Depending upon the goal of a particular model, the mechanisms which must be addressed in the modeling of a solidification process may vary considerably. In general, the issues involved can be divided into two classes. At the macroscopic level, the transport of heat and solute govern the conditions which are present at the advancing interface. These are handled with the appropriate differential equations which can be discretized and solved using various techniques. At the microscopic level, the response of the interface to the instantaneous conditions must be described. This includes the motion of the interface and the associated redistribution of heat and solute. In recent years, various phase-field[1-6] and cellular automaton (CA)[7-14] models have been used to simulate many features of dendritic solidification.

Phase-field methods involve describing the interface with one or more order parameters which may vary continuously between two constant values, indicating the respective phases. The energy or entropy of the system is described in Cahn-Hilliard fashion using a double-well potential with minima associated with the solid and liquid values of the order parameters. The evolution of the continuous phase-field is governed by the dissipation of energy or by the production of entropy. These methods have been used to successfully model many aspects of dendritic solidification at the microscopic level.[1-6] The technique is computationally limited, however, by the requirement of an

Mat. Res. Soc. Symp. Proc. Vol. 529 © 1998 Materials Research Society

interface which is both very thin and well resolved. In some cases, this limitation does not permit the implementation of realistic conditions.

Cellular automata are discrete lattice, rule-based growth algorithms developed to study the evolution of self-organizing systems of identical components. The utility of these methods is only beginning to be appreciated, and the use of automata for solidification modeling has been limited. The CA technique was first applied to the phenomenon of dendritic crystal growth in 1985 by Packard.[7] This model produced equiaxed dendritic shapes in two dimensions for a pure substance by considering heat flow, interface curvature, and latent heat generation. Brown and Spittle[8] simulated the formation of dendritic grain structures in a pure metal by assuming an initial distribution of nuclei and using a Monte-Carlo algorithm for further nucleation and growth. Growth was based on minimization of energy, which included a bulk term for each phase and an interfacial term. By varying the boundary conditions, the qualitative effects of melt superheat and mold temperature on the columnar to equiaxed transition, were reproduced. In a subsequent model, which was a direct extension of the original Packard model, the evolution of dendrite morphology in an initially uniformly undercooled pure metal was simulated.[9] Rappaz and Gandin have modeled the formation of grain structures during solidification by using a CA growth algorithm based on a prescribed growth relationship governing the dendrite tip kinetics, where the velocity is an explicit function of the temperature. Thus, by assuming that all growth is fully dendritic, the growth of the dendrite envelope is modeled by tracking only the tips. The CA for growth is coupled to a finite element (FE) thermal calculation which allows for the liberation of heat based on a solid fraction-temperature function, truncated at the temperature of the dendrite tip. The temperature at each tip is obtained from the FE calculation and used by the CA algorithm to update the shape of the solid. By incorporating various aspects of nucleation and fluid flow, several features of solidification structures have been modeled quantitatively.[10-15]

In previous work by the authors, a cellular automaton approach has been used to mimic morphological instability and to simulate dendritic solidification structures for a range of directional growth conditions.[16,17] Additionally, it has been shown that anisotropic configurational parameters are necessary to produce stable dendritic morphologies.[17] The objective of the current work is to advance this approach by exploring the effects of a configurational term for kinetic anisotropy.

MODEL DESCRIPTION

The simulation domain is a square mesh where each cell is assigned a value for temperature, composition, and phase. Temperature and composition are continuous field variables while the phase is a discrete binary variable. The overall operation of the model involves coupling the evolution of the temperature and solute field with the motion of the phase boundary. The solute field is updated using an alternate-direction-implicit finite-difference (ADI-FD) method with periodic lateral boundaries. For the simulations presented here, the thermal field is specified as either directional or uniform. The uniform conditions are implemented by imposing a fixed cooling rate on a field of uniform temperature. Conditions for directional solidification are implemented by employing a uniform temperature gradient and a constant isotherm velocity. In the directional case, the simulation frame is permitted to move in order to follow the front over distances much greater than the domain itself.

The morphology of the solid is evolved using a CA technique which is intended to simulate the morphological evolution of an advancing solidification front by including the relevant physical factors such as temperature, composition, and interface curvature. The contribution from each is incorporated into a growth function which can be applied to every cell within the domain. Each cell is, thus, free to grow as the local conditions allow, and no explicit distinction is made for dendrite

tips or other features. The morphology is updated by comparing random numbers to a growth probability $p(\phi)$, where ϕ is a growth potential computed from the local temperature, composition, and morphology. This method naturally imparts a random noise component to the structure, facilitating the fluctuations necessary to initiate morphological changes. The function p, which is essentially a velocity function, must be bounded by zero and one and should vary monotonically with the growth potential, ϕ. The following function is chosen:

$$p = 1 - \exp[-(\frac{\phi}{\kappa})^{\eta\kappa}] \tag{1}$$

where κ and η can be used to control the shape of the function over the potential domain. The defining characteristics of the model, therefore, are the formulation of the potential ϕ and the description of the constants η and κ, in terms of the physical properties of the alloy.

For a site at position *(i,j)*, the growth potential at time k is defined as the kinetic undercooling:

$$\phi_{ij}^{k} = \Delta T - (\Delta T_C + \Delta T_R) \tag{2}$$

where ΔT is the total undercooling, and the subscripts C and R indicate compositional and curvature related contributions, respectively. With knowledge of the phase diagram, ΔT_C at any cell can be calculated based on the local temperature and composition. With a configurational term for ΔT_R, (2) becomes:

$$\phi_{ij}^{k} = T_m - mC_{ij}^{k} - f(S_{ij}^{k}) - T_{ij}^{k} \tag{3}$$

where T_m is the melting temperature, m is the liquidus slope, C_{ij}^{k} is the solute concentration, T_{ij}^{k} is the temperature, and S_{ij}^{k} is the configuration of the neighborhood about cell *(i,j)* at time k. The configurational contribution to undercooling is computed as:

$$f(S_{ij}^{k}) = \Gamma \frac{(\alpha_r H_r + \alpha_a H_a + \beta)^{\xi}}{\Delta z} \tag{4}$$

where Γ is the Gibbs-Thompson coefficient, β and ξ are modeling constants, and Δz is the grid resolution. The H_i values are contributions due to interfacial curvature (i=r) and anisotropy (i=a), weighted by the coefficients α_r and α_a, respectively. In terms of the first and second nearest neighbors, these can be expressed as follows.

$$H_r = 2 * [\omega(2-\epsilon_1) + (1-\omega)(2-\epsilon_2)] \tag{5}$$

$$H_a = (\epsilon_1-2)\delta(\epsilon_1,\epsilon_2) + (\epsilon_1-\epsilon_2)[\epsilon_2 - 2H'(\epsilon_2-2)]$$

where ω is a weight factor between 0 and 1, ϵ_i is the number of solid i^{th} nearest neighbors, δ is the Kronecker delta, and H' is the Heavyside function.

At this point, we have a method for moving the interface based on the local value of ϕ, which can be computed from the field variables and solid morphology. To determine the kinetic resistance imparted by (1), we evaluate $dp/d\phi$ at a characteristic undercooling of κ.

$$\left.\frac{dp}{d\phi}\right|_{\kappa} = \frac{\eta}{\exp(1)} \equiv \eta' \tag{6}$$

Generally, the velocity of an interface is related to the kinetic undercooling through a proportionality constant:

$$V = M\Delta T \tag{7}$$

where,

$$M = J_o \nu \frac{\Delta s_f}{RT} \exp(\frac{-Q}{RT})$$

J_0 is vibrational frequency, ν is atomic volume, Q is activation energy for diffusion, R is the gas constant, and Δs_f is the entropy associated with solidification.[18] In the model, the velocity is given by the product of the growth probability, the time step frequency, and the cell size of the grid:

$$V = p \frac{\Delta z}{\Delta t} = pV_{max} \tag{8}$$

where V_{max} is the limiting velocity. Combining (6) and (7):

$$p = \frac{M\Delta T}{V_{max}} \tag{9}$$

Considering (1) and (8), η' can be computed by relating the differentials:

$$\eta' = \frac{dp}{d\phi} = \frac{dp}{d(\Delta T)} = \frac{M}{V_{max}} \tag{10}$$

We now have a technique for calculating the value of p at each cell, based on the relevant physical parameters. To update the solid morphology, a random number ($0 \le r \le 1$) is generated for each cell at each time step for comparison with p. If $p_{ij}^k > r_{ij}^k$, the cell is set to solid. The composition is then set to kC_{ij}^k, and the excess solute $(1-k)C_{ij}^k$ is distributed among the available neighboring cells.

MODELING RESULTS

All results presented in this section were obtained using input parameters associated with Al-4.5 wt% Cu. The effect of the anisotropic contribution was explored by examining the growth of a single seed in the center of a uniform melt which is cooled at a constant rate. The grid resolution for these calculations is 1.5×10^{-5} m. The initial seed is circular in shape, with a diameter of 3.0×10^{-4} m. The effect of H_a on the evolution of growth shape from the seed is shown for three different values of H_a in Figure 1. In Figure 1a, the value of H_a is not sufficient to overcome the anisotropy introduced by the grid, which dictates the initial square growth shape. For this shape, diffusive effects at the corners promote rapid growth and the shape evolves as shown. In Figure 1b, the value of H_a is high enough to result in an initial growth shape with {11} interfaces. Once again, the corners grow rapidly and the shape evolves into a dendritic structure with side branches. In Figure 1c, the value of H_a is, again, high enough to promote {11} interfaces in the initial growth shape. As the shape evolves, however, it becomes clear that H_a is so high that other orientations have been almost completely suppressed, resulting in unnatural structures. A more advanced stage of morphological evolution for the intermediate value of H_a is shown in Figure 2.

In the case of directional growth, the effect of the anisotropy parameter is equally important. Figure 3 shows the initial structural evolution during directional growth, using three different values for H_a. For H_a=0.1, the anisotropy imparted by the grid promotes {01} interfaces. This suppresses the development of curved cell tips. Cell fronts remain relatively flat until the undercooling becomes

high enough to overcome the grid effect. This results in an abrupt and unnatural transition in morphology during the evolution of the dendritic front, as shown in Figure 3a. For H_a=0.3, the structure is no longer dominated by {01} interfaces, and it evolves smoothly into a dendritic front, as shown in Figure 3b. When H_a is increased further to a value of 0.5, as in Figure 3c, the {11} interfaces dominate the structure, resulting in pointed dendrite tips. Figure 4 shows the near-steady-state morphology resulting from directional growth using the intermediate value of H_a.

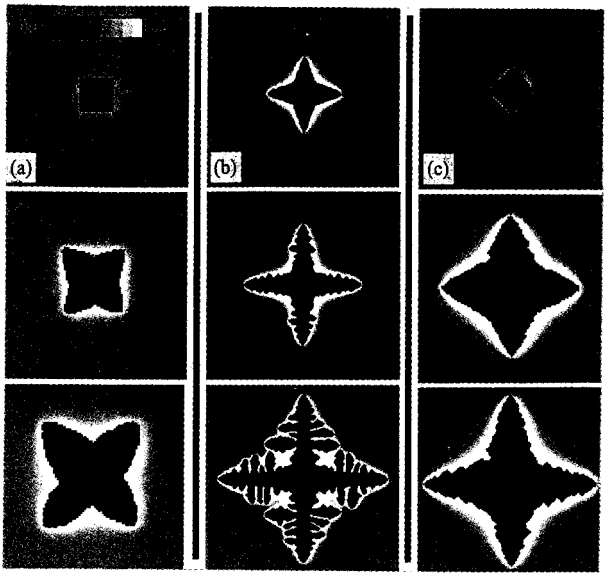

Figure 1. A comparison between simulated growth morphologies for a circular seed in a uniform melt: (a) Hs=0.1, (b) Hs=0.3, (c) Hs=0.5. Domain = 3 x 3 mm. Mesh = 200 x 200.

CONCLUSIONS

The anisotropy imparted by the grid has a significant effect on the resulting morphology. The incorporation of kinetic anisotropy, even through a simple configurational term, is essential for the simulation of realistic dendritic patterns using a cellular automaton approach.

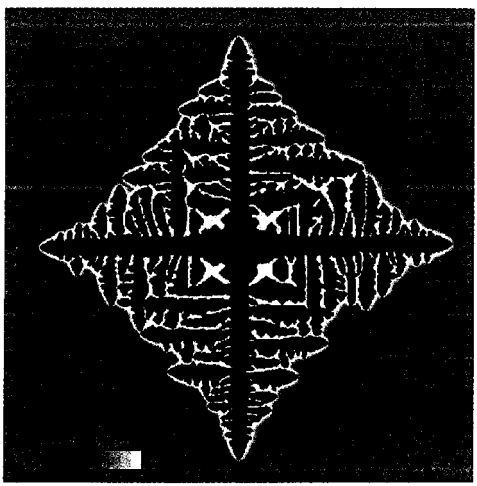

Figure 2. Later stage of growth for the simulation shown in Figure 1b. Domain = 6 x 6 mm. Mesh = 400 x 400.

REFERENCES

1. R. Kobayashi; *Physica D*, **63** (1993) 410-423.
2. A.A. Wheeler, B.T. Murray, and R.J. Schaefer; *Physica D*, **66** (1993) 243.
3. S.L. Wang, R.F. Sekerka, A.A. Wheeler, B.T. Murray, S.R. Coriell, R.J. Braun, and G.B. McFadden; *Physica D*, **69** (1993) 189-200.
4. A.A.Wheeler, W.J. Boettinger, and G.B. McFadden; *Physical Review E*, **47** (1993) 1893.
5. J.A. Warren and W.J. Boettinger; *Acta Metall. Mater.*, **43** (1995) 689-703.

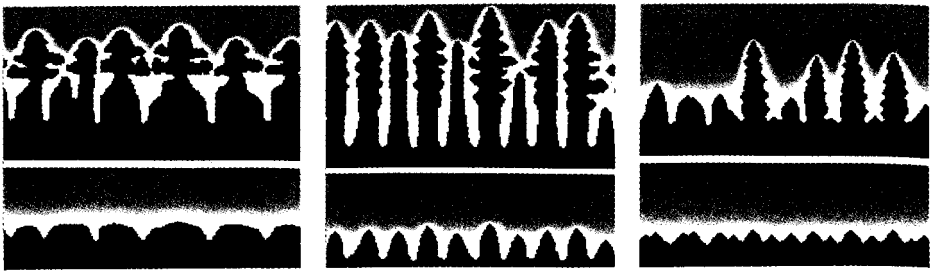

(a) (b) (c)

Figure 3. A comparison between simulated morphologies developing from a flat seed along the boundary, with directional cooling conditions: (a) Hs=0.1, (b) Hs=0.3, (c) Hs=0.5. Domain = 3 x 3 mm. Mesh = 200 x 200.

6. W.J. Boettinger and J.A. Warren; *Met. Mater. Trans.*, **27A** (1996) 657-669.
7. N.H. Packard; *Proceedings of the First Int. Symposium for Science on Form*, (Y. Katoh, R. Takaki, J. Toriwaki, and S. Ishizaka, Eds.), KTK Scientific Publishers (1986).
8. S.G.R. Brown and J.A. Spittle; *Scripta Metallurgica*, **27** (1992) 1599-1603.
9. S.G.R. Brown, T. Wiliams, and J.A. Spittle; *Acta Metall. Mater.*, 42 (1994) 2893-2898.
10. M. Rappaz and Ch.-A. Gandin; *Acta Metall. Mater.*, **41** (1993) 345-360.
11. Ch.A. Gandin, M. Rappaz, and R. Tintillier; *Met. Trans.*, **24A** (1993) 467-479.
12. Ch.A. Gandin, M. Rappaz, and R. Tintillier; *Met. Trans.*, **25A** (1994) 629-635.
13. M. Rappaz, Ch.A. Gandin, and R. Sasikumar; *Acta Metall. Mater.*, **42** (1994) 2365-2374.
14. Ch.-A. Gandin and M. Rappaz; *Acta Metall. Mater.*, **42** (1994) 2233-2246.
15. Ch.-A. Gandin, Ch. Charbon, and M. Rappaz, *ISIJ International*, **35** (1995) 651-657.
16. R.E. Napolitano and T.H. Sanders, Jr., *Proc. Int. Symp. on Processing of Metal and Advanced Materials: Modeling, Design, and Properties*; B.Q. Li, E d., TMS (1998) 63-74.
17. R.E. Napolitano and T.H. Sanders, Jr., Proc. *Third Pacific Rim International Conference on Advanced Materials and Processing*; TMS (1998).
18. K.A. Jackson, *Journal of Crystal Growth*, 3/4 (1968) 507-517.

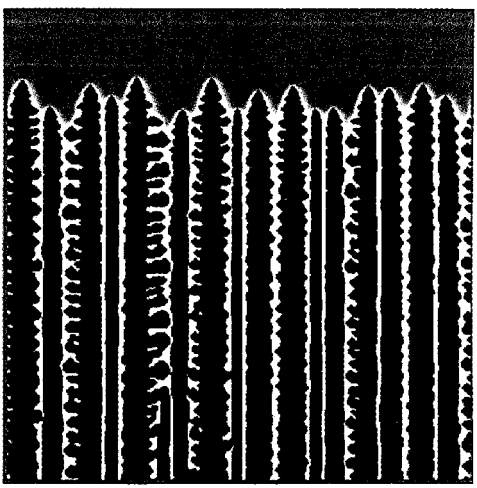

Figure 4. Later stage of growth for the simulation shown in Figure 3b. Domain = 6 x 6 mm. Mesh = 400 x 400